

Facile fractionation of lignocelluloses by biomass-derived deep eutectic solvent (DES) pretreatment for cellulose enzymatic hydrolysis and lignin valorization

Xiao-Jun Shen ^{a,b,c}, Jia-Long Wen ^{a*}, Qing-Qing Mei ^{b,c}, Xue Chen^a, Dan Sun^a Tong-

Qi Yuan ^a, Run-Cang Sun ^{a*}

^aBeijing Key Laboratory of Lignocellulosic Chemistry, Beijing Forestry University, Beijing 100083, P. R. China

^bBeijing National Laboratory for Molecular Sciences, Key Laboratory of Colloid and Interface and Thermodynamics, Institute of Chemistry, Chinese Academy of Sciences, Beijing 100190, P. R. China.

^cUniversity of Chinese Academy of Sciences, Beijing 100049, P. R. China.

*Corresponding authors: J.L. Wen; R.C. Sun.

Address: Beijing Key Laboratory of Lignocellulosic Chemistry, Beijing 100083, China.

E-mail address: rcsun3@bjfu.edu.cn (R.C. Sun); wenjialong@bjfu.edu.cn (J.L. Wen)

Content

1. Material and methods.....	5
------------------------------	---

1.1 Preparation of DES	5
1.2. Characterization of the DES	5
1.3. Characterization of the lignin fractions	5
1.4. Structure elucidation of the cellulose-rich substrates	6
1.5. Enzymatic hydrolysis.....	7
2. Tables and Figures	8
Table S1. Pulp yield and its composition as well as precipitated lignin yield obtained under different pretreatment temperatures.....	8
Table S2: Pulp yield and its composition as well as the yield of the precipitated lignin obtained at different DES ratios.	9
Table S3. The NMR assignments of major components in the HSQC spectra of original and the pretreated substrates.....	10
Table S4: Pulp yield and its composition as well as the precipitated lignin yield during recyclability experiment	11
Table S5. Acidity (pH value) of DES solution before and after recyclability process.....	12
Figure S1. Chemical compositions of original and the pretreated substrates under different pretreatment temperatures	13
Figure S2. The viscosity curves of the fresh and the recycled DES after different pretreatment temperature.	14
Figure S3. Recovery yield of solid, cellulose, lignin and hemicelluloses at different DES ratios.	15
Figure S4. Chemical compositions of original and the pretreated substrates under different ratios DES pretreatment.....	16
Figure S5. X-ray diffraction of original and the pretreated substrates under different pretreatment temperatures.	17
Figure S6. X-ray diffraction of original and the pretreated substrates at different ratios of DES pretreatment.	18
Figure S7. SEM images of the original and pretreated substrates under different ratios of DES pretreatment.	19
Figure S8. Glucose yields of enzymatic hydrolysis of original and the pretreated substrates at different ratio of DES pretreatment.	20
Figure S9. Trends for lignin removal and lignin yield in relation to saccharification yield under different DES pretreatment temperatures.	21
Figure S10. Side-chain region in the 2D-HSQC NMR spectra of DEL and the lignins obtained under different ratio of DES pretreatment.	22

Figure S11. Aromatic region in the 2D HSQC NMR spectra of DEL and the lignins obtained under different ratio of DES pretreatment.	23
Figure S12. Main classical substructures, involving different side-chain linkages, and aromatic units identified by 2D NMR of residual lignin (<i>Eucalyptus</i>): (A) β -O-4 aryl ether linkages with a free -OH at the γ -carbon; (A') acetylated β -O-4 aryl ether linkages with lactic acid at the γ -carbon; (B) resinol substructures formed by β - β , α -O- γ , and γ -O- α linkages; (C) phenylcoumarane substructures formed by β -5 and α -O-4 linkages; (I) <i>p</i> -hydroxycinnamyl alcohol end-groups; (H) <i>p</i> -hydroxyphenyl units; (G) guaiacyl units; (G') oxidized syringyl units with a C $_{\alpha}$ ketone; (S) syringyl units; (S') oxidized syringyl units with a C $_{\alpha}$ ketone.	24
Figure S13. Chemical compositions of the original and pretreated substrates under different pretreatment cycle times.	25
Figure S14. X-ray diffraction of original and the pretreated substrates under different pretreatment cycle times.	26
Figure S15. SEM images of original and the pretreated substrates under different pretreatment cycle times.	27
Figure S16. Inhibitors and monosaccharides in the DES solution after the different pretreatment temperatures.	28
Figure S17. Side-chain in the 2D HSQC NMR spectra of DEL and the lignins obtained under different pretreatment cycles.	30
Figure S18. Aromatic region in the 2D HSQC NMR spectra of DEL and the lignins obtained under different pretreatment cycles.	31
Figure S19. ¹ H NMR spectra of fresh and the recycled DES at different DES cycles.	32
Figure S20. ¹³ C NMR spectra of fresh and the recycled DES at different DES cycles.	33
Figure S21. 2D-HSQC NMR spectra of fresh and the recycled DES at different DES cycles.	34
Figure S22. ¹ H NMR spectra of fresh and the recycled DES under different pretreatment temperatures.	35
Figure S23. ¹ H NMR spectra of fresh and the recycled DES at different DES ratio.	36
Figure S24. ¹³ C NMR spectra of fresh and the recycled DES under different pretreatment temperatures.	37
Figure S25. ¹³ C NMR spectra of fresh and the recycled DES at different DES ratio.	38
Figure S26. Side-chain and aromatic region in the spectra of pure DES and the recycled DES under different pretreatment temperatures.	39
Figure S27. Side-chain and aromatic region in the 2D HSQC NMR spectra of pure DES and the recycled DES under different DES ratio.	40

1. Material and methods

1.1 Preparation of DES

Choline chloride (ChCl) was mixed with lactic acid to obtain the DES. The binary mixtures with different molar ratio of (1:10 and 1:5) were allowed to react under reduced pressure at 80 °C until solid particles were disappeared. Once the homogeneous and transparent liquid was formed, the mixture was cooled down in a desiccator to room temperature to avoid moisture absorption.

1.2. Characterization of the DES

The viscosity of DESs was measured on a Brookfield digital Viscometer DV-II PRO (Brookfield Instruments, America) using S34 rotor with a speed of 5.0 rpm. The ¹H and ¹³C NMR as well as 2D-HSQC NMR spectra of the prepared DES were acquired. The pH value of the DES was measured by diluting 1 ml DES solution obtained either fresh or after four uses with 9 ml deionized water. The pH of the diluted solution was measured using pH meter equipped.

The contents of xylose, arabinose, mannose, rhamnose, galactose, glucose, furfural, hydroxymethylfurfural (HMF), acetic acid, formic acid, levulinic acid and lactic acid in the DES solution after pretreatment were determined according to the analytical method (NREL/TP-510–42623) (Sluiter et al., 2008a).

1.3. Characterization of the lignin fractions

The weight-average (M_w) and number-average (M_n) molecular weights of the lignin samples were determined by gel permeation chromatography (GPC) (Agilent

1200, Agilent Technologies, USA) with an ultraviolet detector (UV) at 240 nm. The column used was a PL-gel 10 mm mixed-B 7.5 mm i.d. column, which was calibrated with PL polystyrene standards according to a previous report (Shen et al., 2016a). NMR spectra of lignin samples were recorded on a Bruker AVIII 400 MHz spectrometer at 25 °C in DMSO-d₆. The quantitative ¹³C NMR and quantitative 2D-HSQC experiments were conducted according to previous literatures (Crestini & Argyropoulos, 1997; Shen et al., 2016a; Wen et al., 2015). ³¹P NMR spectra were acquired according to previous literatures (Crestini & Argyropoulos, 1997; Pu et al., 2011; Shen et al., 2016a; Wen et al., 2015).

1.4. Structure elucidation of the cellulose-rich substrates

The chemical compositions (% w/w) of the cellulose-rich substrates were determined according to the NREL standard analytical method (NREL/TP-510-42618) (Sluiter et al., 2008b). The cellulose, hemicelluloses and lignin recovery were calculated as previously (Shen et al., 2016b). The microstructural changes and surface characteristics of the different cellulose-rich substrates were analyzed with a scanning electron microscope (SEM) (S-3400N II, HITACHI Company, Japan) operating at 10 kV acceleration voltages. All samples were coated with gold prior to acquiring images. The diffraction patterns were measured from 2° to 45° at a scanning speed of 2°/min. The crystallinity index (CrI) was calculated by the peak height method (Segal et al., 1959).

$$\text{CrI} = \frac{I_{002} - I_{\text{am}}}{I_{002}} \times 100\%$$

Where the I_{002} is the intensity of 002 lattice diffraction ($2\theta = 22.6^\circ$) and the I_{am} is the intensity of amorphous section ($2\theta = 18^\circ$).

1.5. Enzymatic hydrolysis

Enzymatic hydrolysis was carried out at 2% of different *eucalyptus* samples (w/v) in 10 mL of 50 mM sodium acetate buffer (pH 4.8) using shaking incubators (ZWYR-2102C) (Shanghai, China) at 150 rpm for 72 h. Cellulase (Cellic@ CTec2, 100 FPU/ml) was provided from novozymes (Beijing, China) and employed at the activity of 15 FPU/g substrate for all the samples. The hydrolysis reaction solution of 200 μ L was sampled at 0, 3, 6, 9, 12, 24, 48, 60, and 72 h. The intermittent sample was sealed and incubated in a boiling water bath for 5 min to terminate the cellulose hydrolysis reaction, and then centrifuged at 10,000 rpm for 5 min to obtain the supernatant. The supernatant (100 μ L) was diluted by ultrapure water, and filtered through a 0.22 μ m filter prior to sugar analysis by a HPAEC system with an integral amperometric detector and CarboPac PA100 (4*250 mm, Dionex) analytical column according to the literature. All the hydrolysis experiments were carried out in duplicates.

2. Tables and Figures

Table S1. Pulp yield and its composition as well as precipitated lignin yield obtained under different pretreatment temperatures

	Pulp Composition ^b								Total pulp yield	Yield of the precipitated lignin
	Glu	Xyl	Ara	Man	Rhm	Gal	ASL	AIL		
Control	38.7	16.7	0.3	1.2	0.3	0.8	5.1	31.7	100	0
90 °C	41.7	10.9	- ^c	1.0	0.1	0.3	4.2	26.0	78.3	6.4
100 °C	42.7	10.9	-	0.8	0.1	0.3	4.1	23.7	75.8	18.5
110 °C	66.8	3.2	-	0.6	-	-	2.5	12.6	48.3	44.8
120 °C	70.3	2.6	-	0.4	-	-	1.8	6.7	45.3	46.9
130 °C	80.4	2.3	-	-	-	-	1.3	5.2	39.7	58.9

^a Reaction condition: 2 g substrate in 20 g DES solution (choline chloride: lactic acid = 1:10), 6 h;

^b Glu: glucan, Xyl: xylan, Ara: araban, Man: mannan, Rhm: rhamnan, Gal: galactan, ASL: acid soluble lignin, AIL: acid insoluble lignin;

^c -: not detected.

Table S2: Pulp yield and its composition as well as the yield of the precipitated lignin obtained at different DES ratios.

	Pulp Composition ^b								Total pulp yield	Yield of the precipitated lignin
	Glu	Xyl	Ara	Man	Rhm	Gal	ASL	AIL		
Control	38.7	16.7	0.3	1.2	0.3	0.8	5.1	31.7	100	0
lactic acid	56.7	5.0	- ^c	0.8	-	-	1.9	18.6	57.3	47.5
DES (1:10)	66.8	3.2	-	0.6	-	-	2.5	12.6	48.3	44.8
DES (1:5)	68.8	1.5	-	1.3	0.2	0.8	3.7	6.8	49.0	65.3

^a Reaction condition: 2 g substrate in 20 g DES solution, 110 °C 6 h;

^b Glu: glucan, Xyl: xylan, Ara: araban, Man: mannan, Rhm: rhamnan, Gal: galactan, ASL: acid soluble lignin, AIL: acid insoluble lignin;

^c -: not detected.

Table S3. The NMR assignments of major components in the HSQC spectra of original and the pretreated substrates

Label	δ_C/δ_H (ppm)	Assignments
C_β	52.4/3.45	$C_\beta-H_\beta$ in phenylcoumaran substructures (C)
B_β	53.5/3.05	$C_\beta-H_\beta$ in β - β (resinol) substructures (B)
$-OCH_3$	55.7/3.65	C-H in methoxyls
A_γ	59.5/3.64	$C_\gamma-H_\gamma$ in β - O -4 substructures (A)
A'_γ	63.0/4.30	$C_\gamma-H_\gamma$ in γ -acylated β - O -4 (A')
C_γ	62.3/3.70	$C_\gamma-H_\gamma$ in phenylcoumaran substructures (C)
I_γ	61.2/4.10	$C_\gamma-H_\gamma$ in cinnamyl alcohol end-groups (I)
B_γ	71.0/3.79–4.16	$C_\gamma-H_\gamma$ in β - β resinol substructures (B)
A_α	71.6/4.83	$C_\alpha-H_\alpha$ in β - O -4 linked to a S units (A)
$A'_{\beta(G)}$	80.8/4.62	$C_\beta-H_\beta$ in β - O -4 linked to G (A')
$A_\beta(G)$	83.9/4.30	$C_\beta-H_\beta$ in β - O -4 linked to G units (A)
$A'_{\beta(S)}$	83.9/4.30	$C_\beta-H_\beta$ in β - O -4 linked to S units (A')
B_α	84.9/4.64	$C_\alpha-H_\alpha$ in β - β resinol substructures (B)
$A_\beta(S)$	85.9/4.11	$C_\beta-H_\beta$ in β - O -4 linked to a S units (A)
C_α	86.8/5.48	$C_\alpha-H_\alpha$ in phenylcoumaran substructures (C)
$S_{2,6}$	104.0/6.72	$C_{2,6}-H_{2,6}$ in syringyl units (S)
$S'_{2,6}$	106.3/7.21	$C_{2,6}-H_{2,6}$ in oxidized S units (S')
G_2	111.0/6.99	C_2-H_2 in guaiacyl units (G)
G_5	114.8/6.68	C_5-H_5 in guaiacyl units (G)
G_{5e}	115.1/6.95	C_5-H_5 in etherified guaiacyl units (G)
G_6	119.1/6.80	C_6-H_6 in guaiacyl units (G)

Table S4: Pulp yield and its composition as well as the precipitated lignin yield during recyclability experiment

	Pulp Composition ^b								Total pulp yield	Yield of the regenerated lignin
	Glu	Xyl	Ara	Man	Rhm	Gal	ASL	AIL		
Control	38.7	16.7	0.3	1.2	0.3	0.8	5.1	31.7	100	0
1st	66.8	3.2	- ^c	0.6	-	-	2.5	12.6	48.3	44.8
2nd	62.1	5.5	-	0.7	-	-	4.2	13.2	54.7	35.7
3rd	60.3	6.1	-	0.7	-	0.1	4.1	13.4	58.1	30.2
4th	55.4	7.2	-	0.8	0.2	0.1	4.2	15.2	65.6	28.1

^a Reaction condition: 2 g substrate in 20 g DES solution (choline chloride: lactic acid = 1:10), 110 °C, 6 h;

^b Glu: Glucan, Xyl: Xylan, Ara: Arabin, Man: Mannan, Rhm: Rhamnan, Gal: Galactan, ASL: Acid soluble lignin, AIL: Acid insoluble lignin;

^c -: not detected.

Table S5. Acidity (pH value) of DES solution before and after recyclability process

	pH
Fresh DES	0.71
Recycled DES (4 th recycle)	0.80

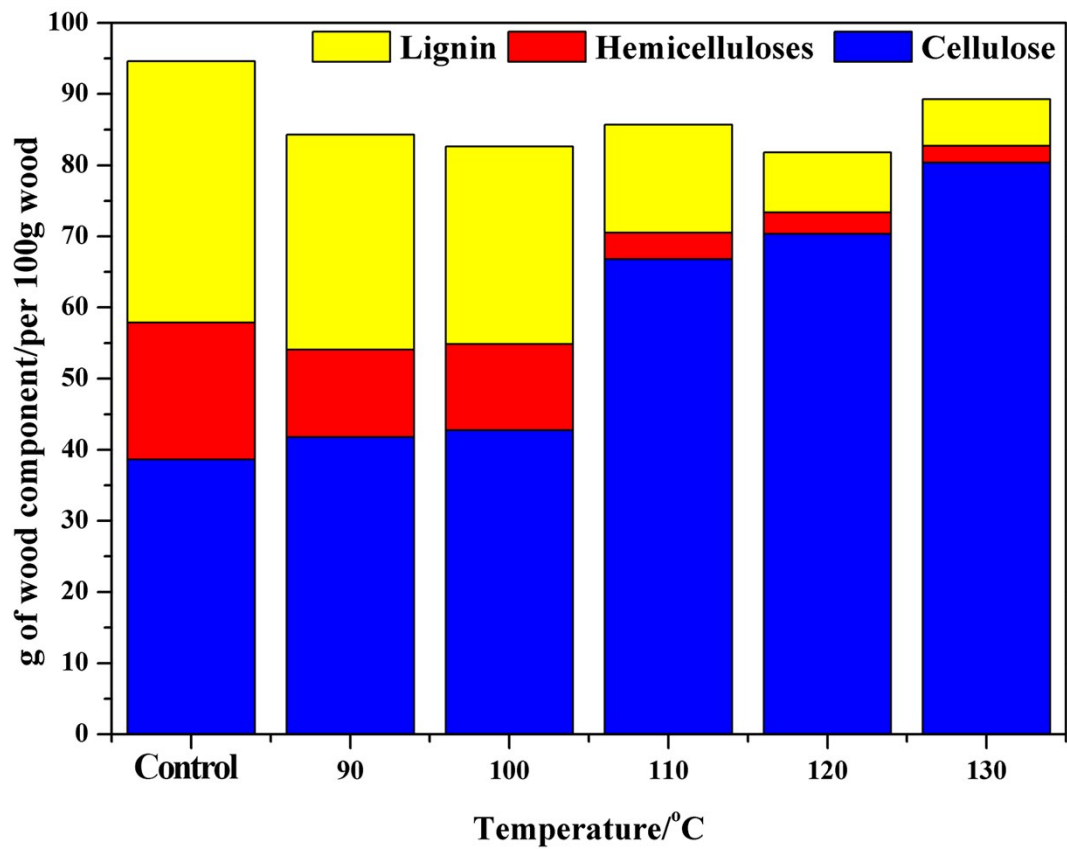


Figure S1. Chemical compositions of original and the pretreated substrates under different pretreatment temperatures

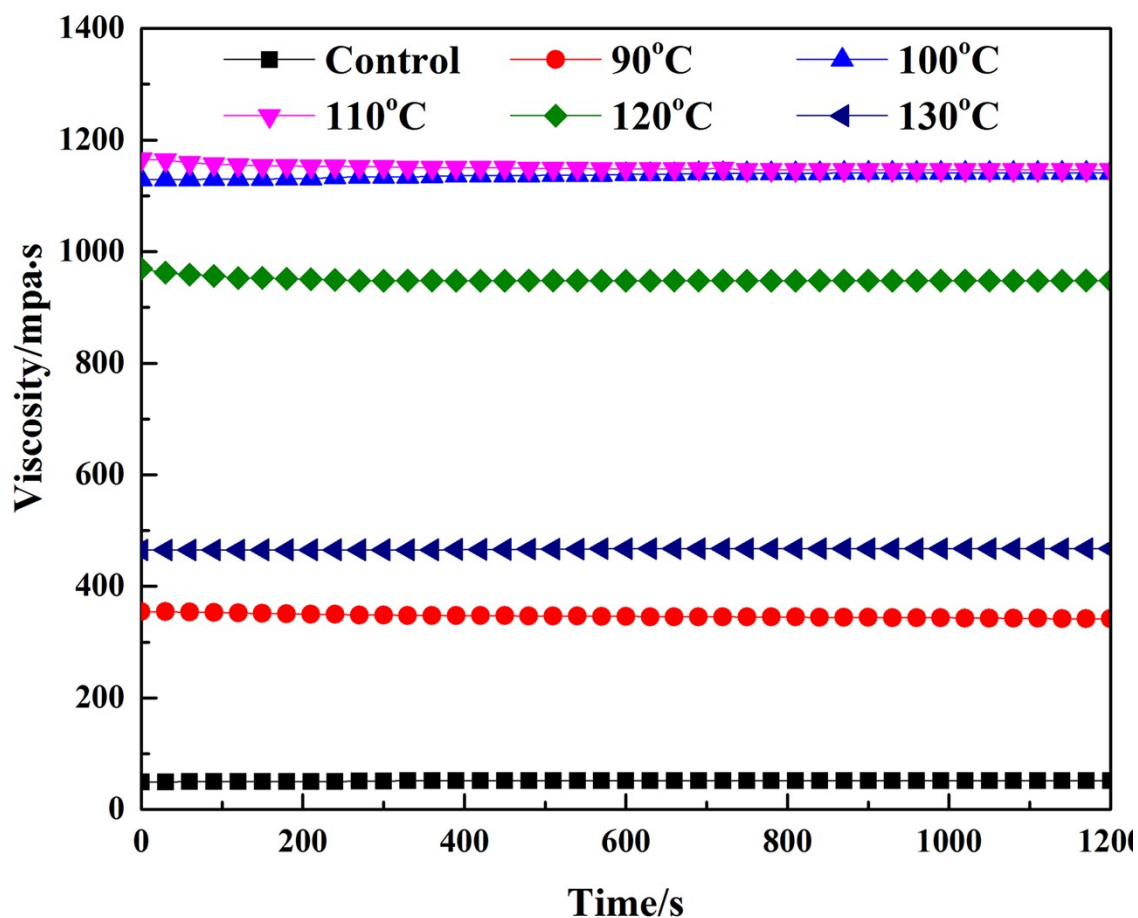


Figure S2. The viscosity curves of the fresh and the recycled DES after different pretreatment temperature.

After the DES pretreatment, the contents of hemicelluloses in the pretreated substrates rapidly decreased with the elevated pretreatment temperature. The released sugars were present as a mixture polyol of oligosaccharides and monosaccharides, which can be also formed DES with ChCl and increased the viscosity of solution (Figure S2). However, when the temperature increased to more than 110 °C, the degradation of polyols (oligosaccharides and monosaccharides) likely occurred. The degradation of polyols will further decrease the viscosity of DES solution.

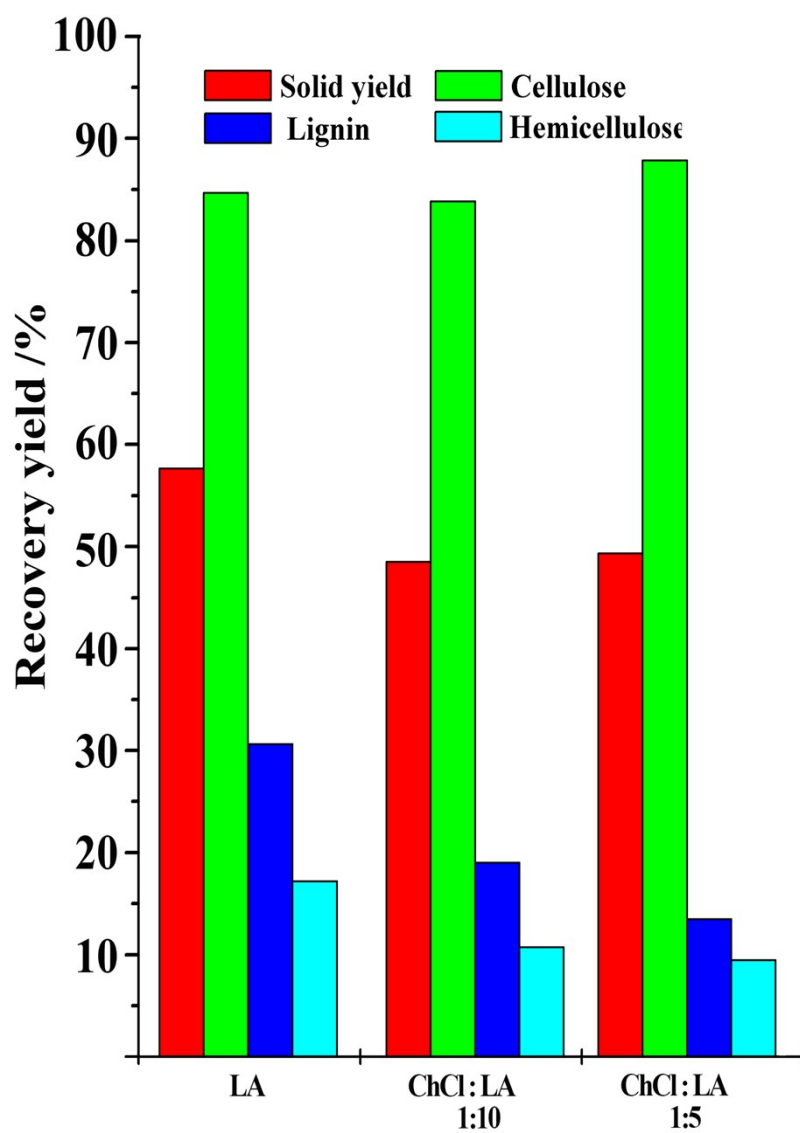


Figure S3. Recovery yield of solid, cellulose, lignin and hemicelluloses at different DES ratios.

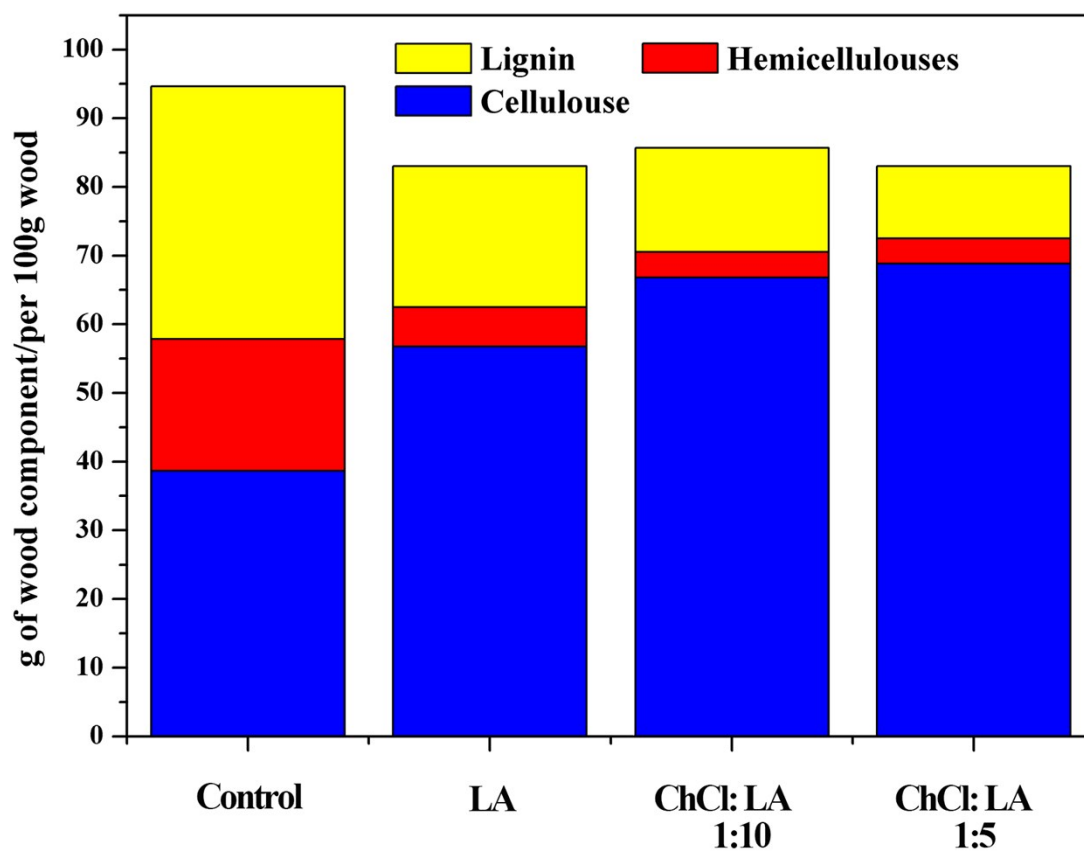


Figure S4. Chemical compositions of original and the pretreated substrates under different ratios DES pretreatment.

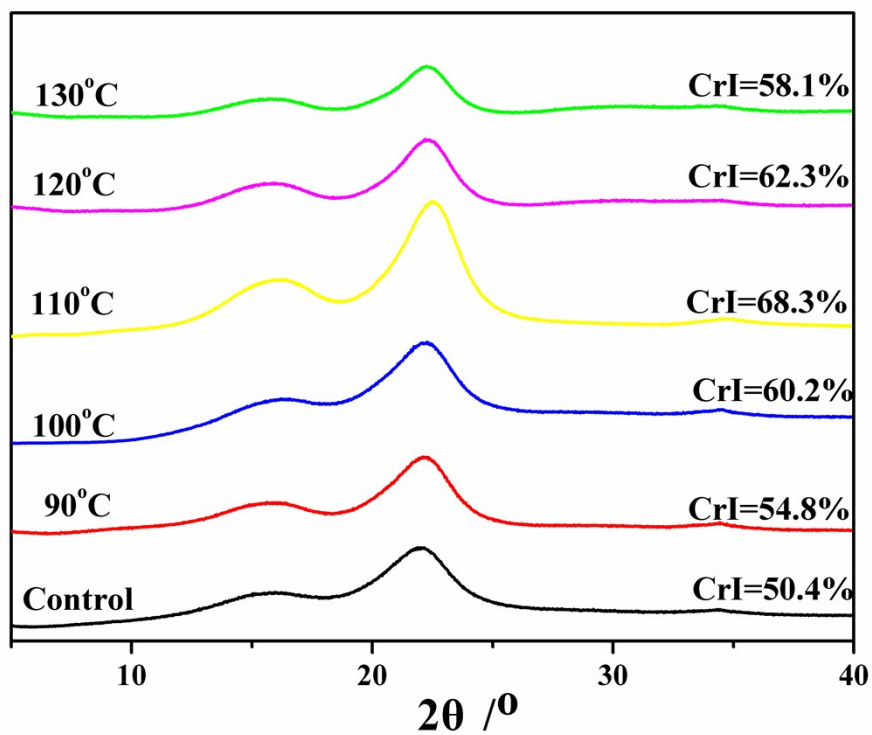


Figure S5. X-ray diffraction of original and the pretreated substrates under different pretreatment temperatures.

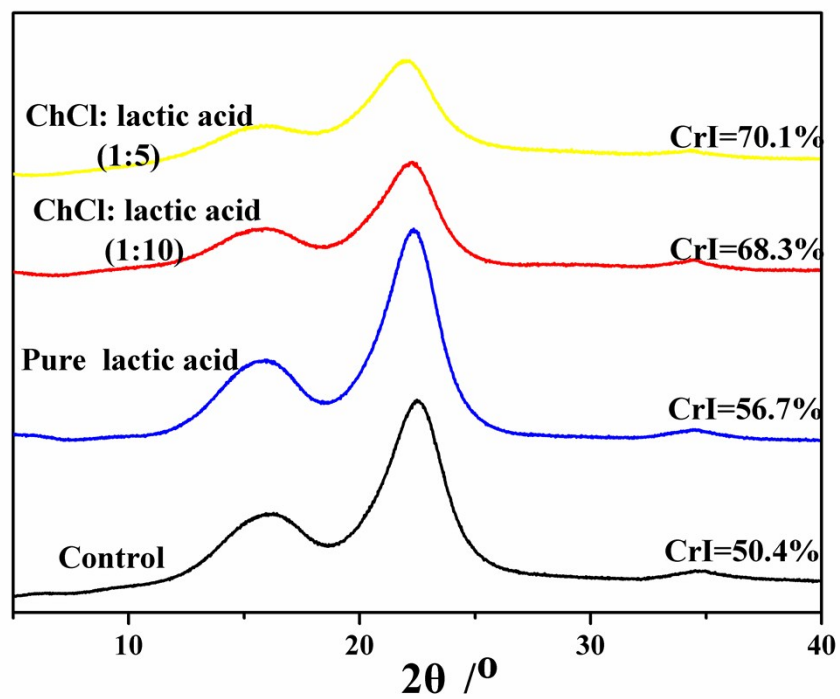


Figure S6. X-ray diffraction of original and the pretreated substrates at different ratios of DES pretreatment.

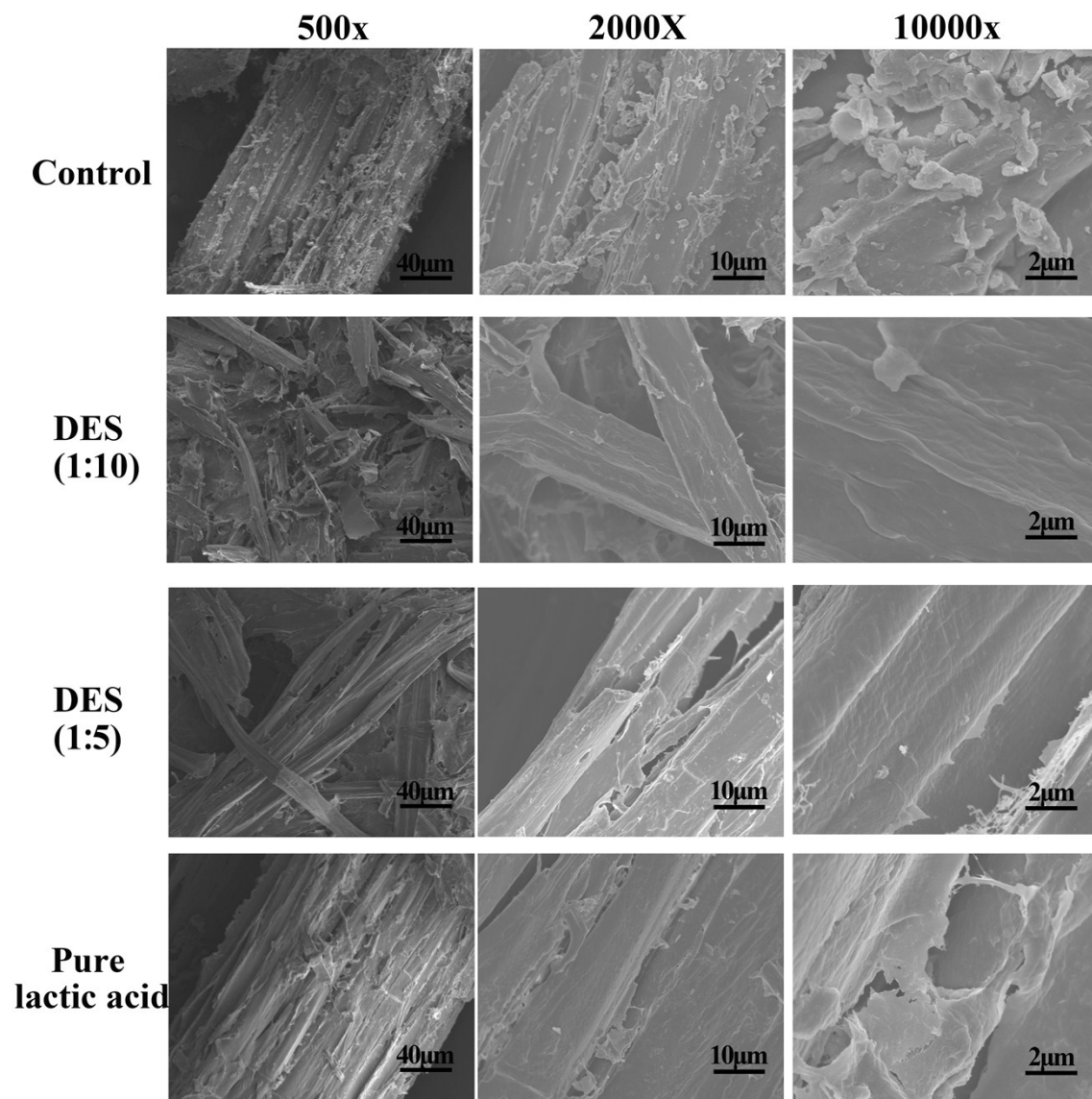


Figure S7. SEM images of the original and pretreated substrates under different ratios of DES pretreatment.

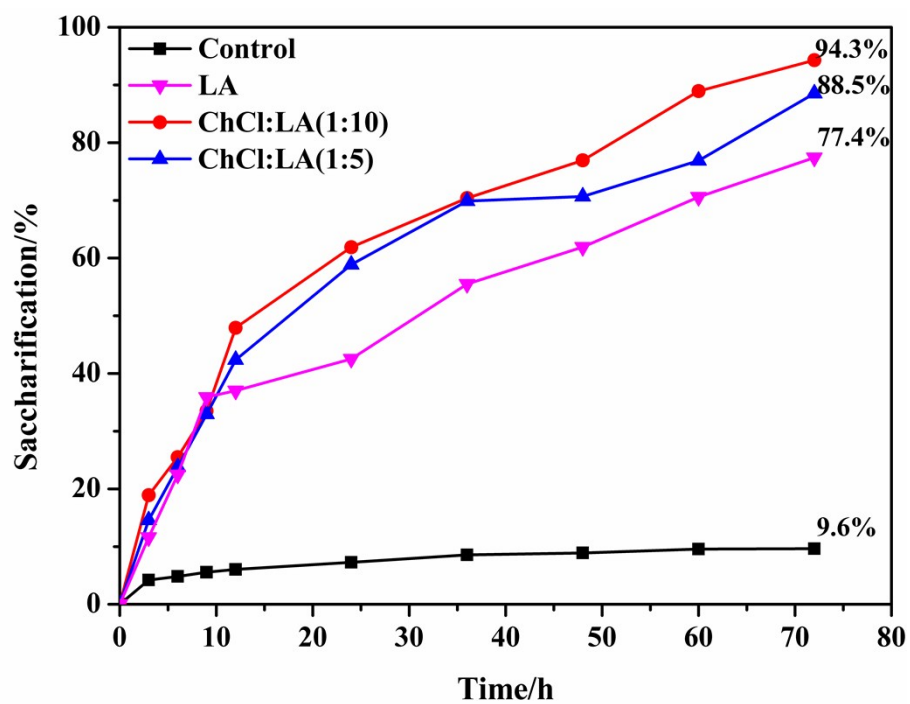


Figure S8. Glucose yields of enzymatic hydrolysis of original and the pretreated substrates at different ratio of DES pretreatment.

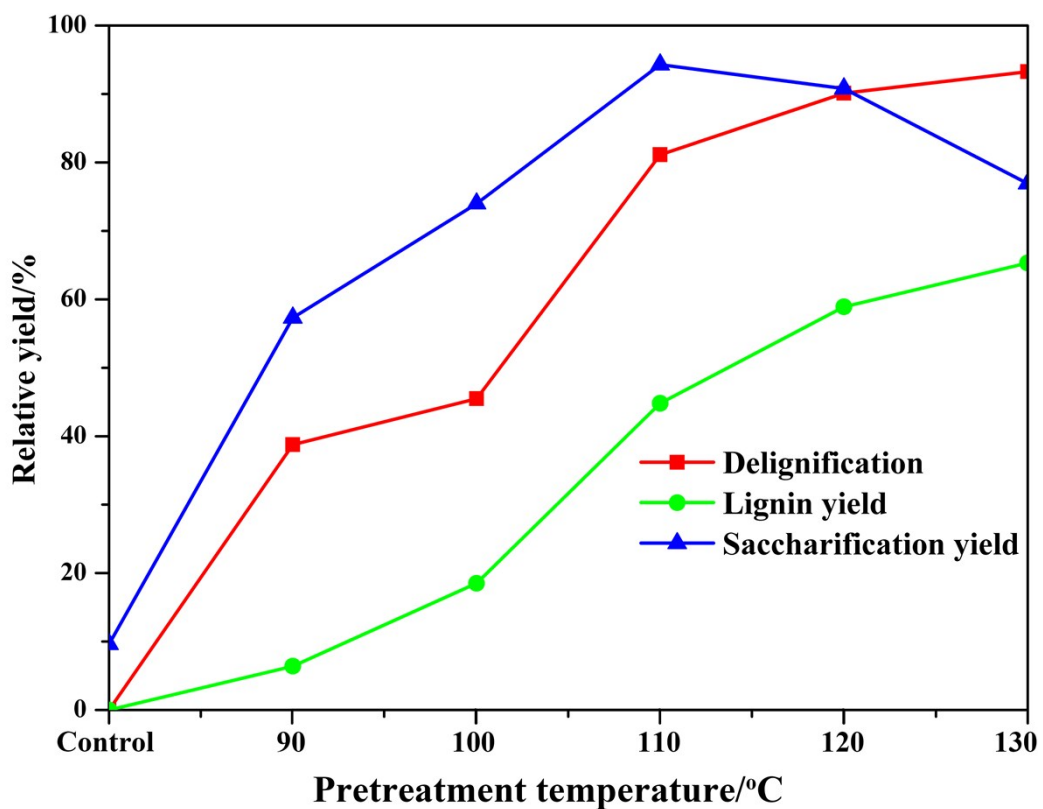


Figure S9. Trends for lignin removal and lignin yield in relation to saccharification yield under different DES pretreatment temperatures.

Note: Delignification=1-Lignin Recovery

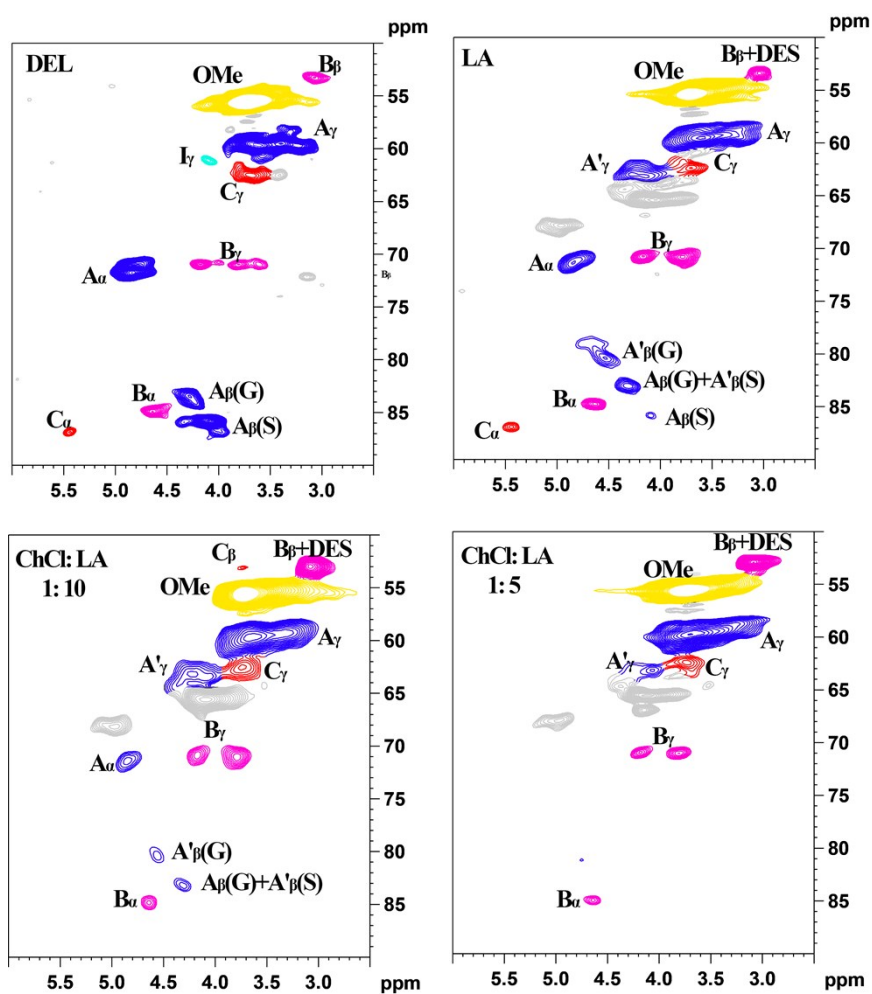


Figure S10. Side-chain region in the 2D-HSQC NMR spectra of DEL and the lignins obtained under different ratio of DES pretreatment.

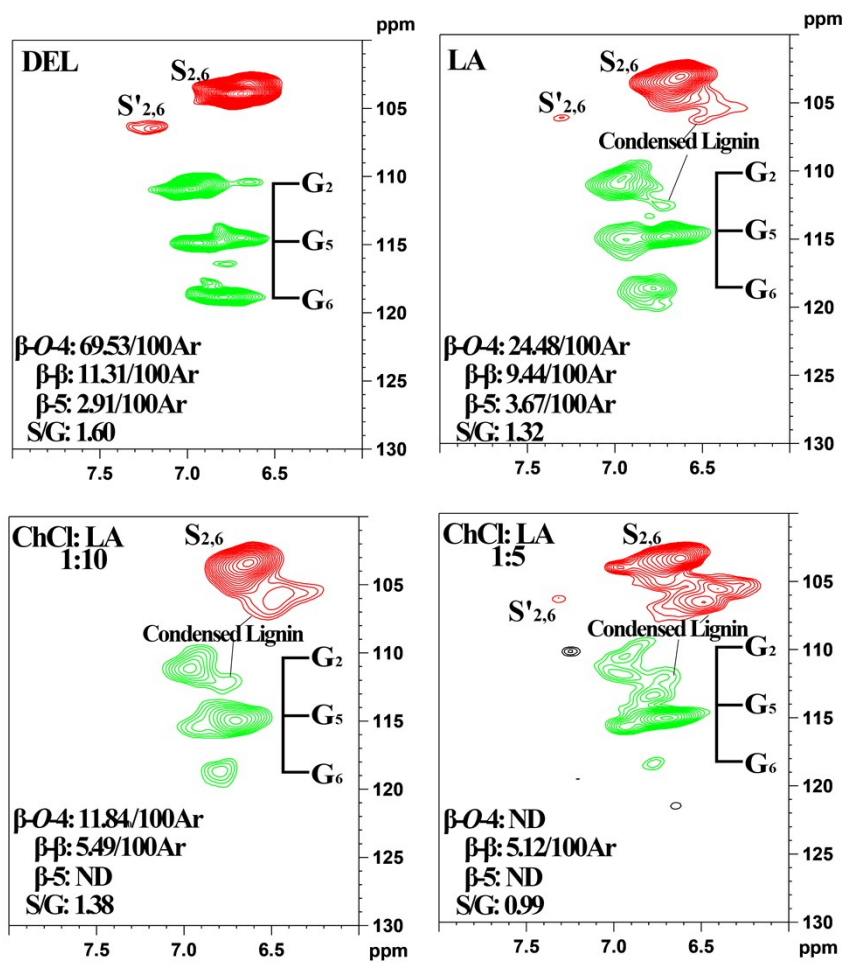


Figure S11. Aromatic region in the 2D HSQC NMR spectra of DEL and the lignins obtained under different ratio of DES pretreatment.

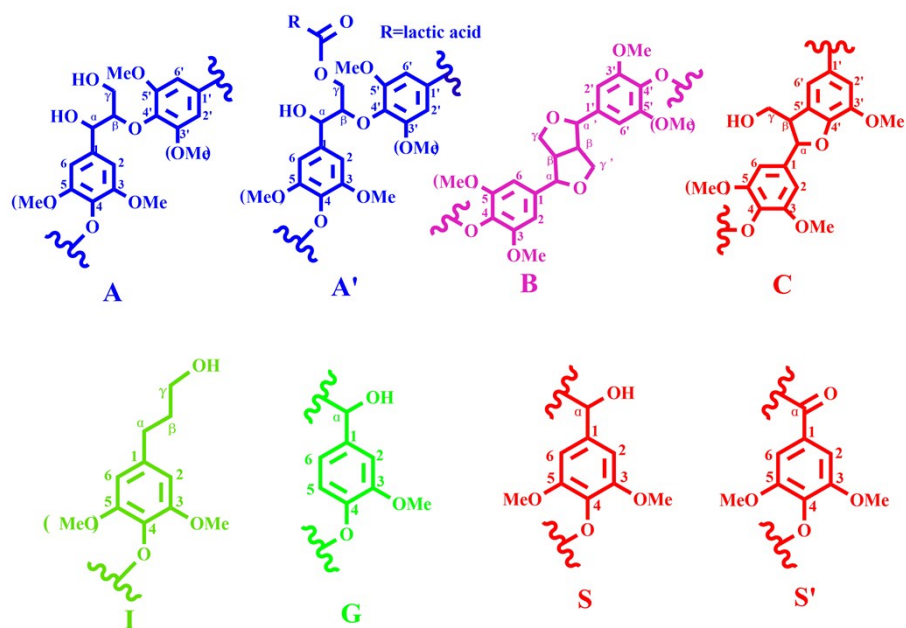


Figure S12. Main classical substructures, involving different side-chain linkages, and aromatic units identified by 2D NMR of residual lignin (*Eucalyptus*): (A) β -O-4 aryl ether linkages with a free -OH at the γ -carbon; (A') acetylated β -O-4 aryl ether linkages with lactic acid at the γ -carbon; (B) resinol substructures formed by β - β , α -O- γ , and γ -O- α linkages; (C) phenylcoumarane substructures formed by β -5 and α -O-4 linkages; (I) *p*-hydroxycinnamyl alcohol end-groups; (H) *p*-hydroxyphenyl units; (G) guaiacyl units; (G') oxidized syringyl units with a C $_{\alpha}$ ketone; (S) syringyl units; (S') oxidized syringyl units with a C $_{\alpha}$ ketone.

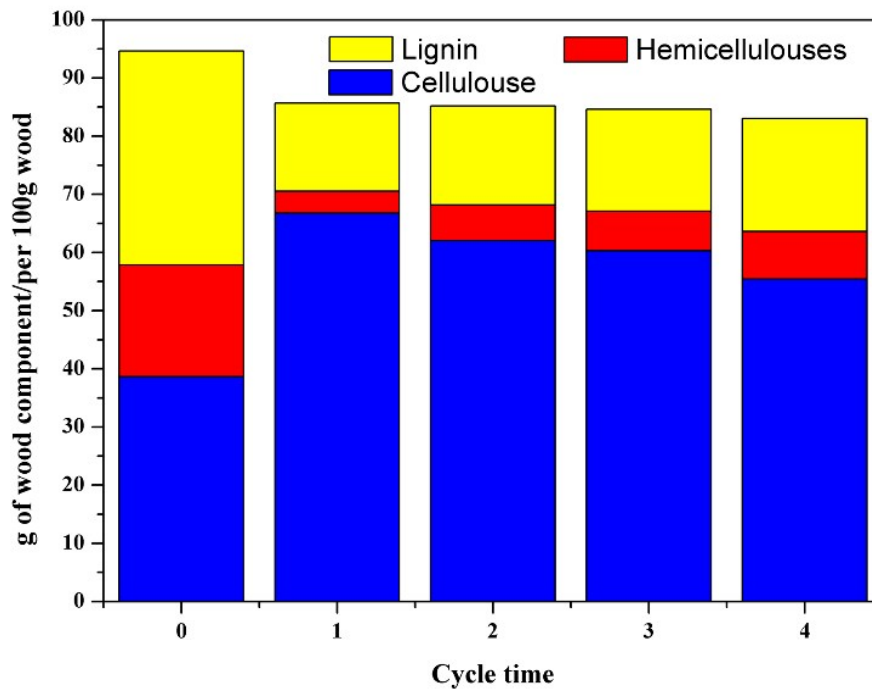


Figure S13. Chemical compositions of the original and pretreated substrates under different pretreatment cycle times

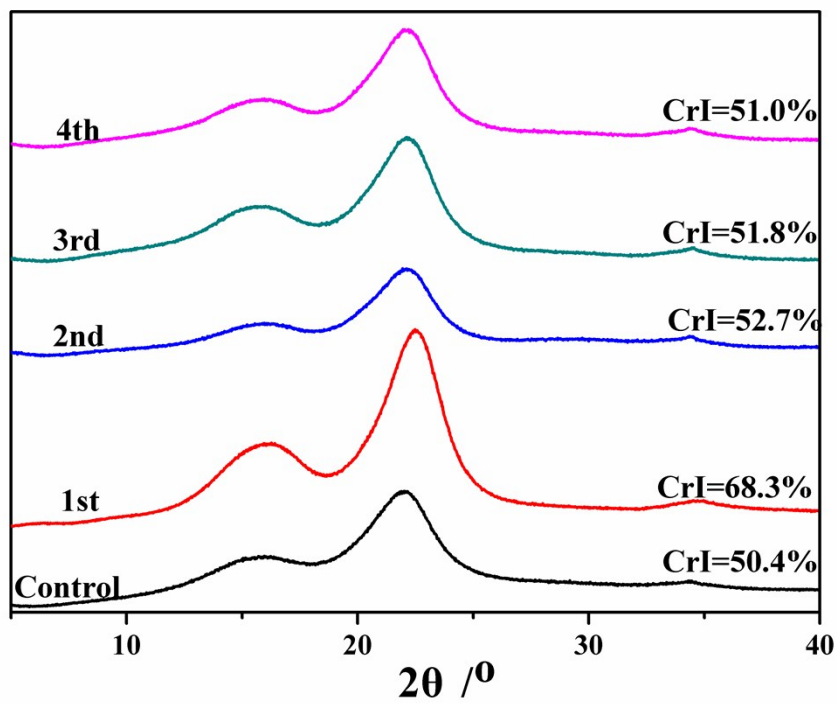


Figure S14. X-ray diffraction of original and the pretreated substrates under different pretreatment cycle times.

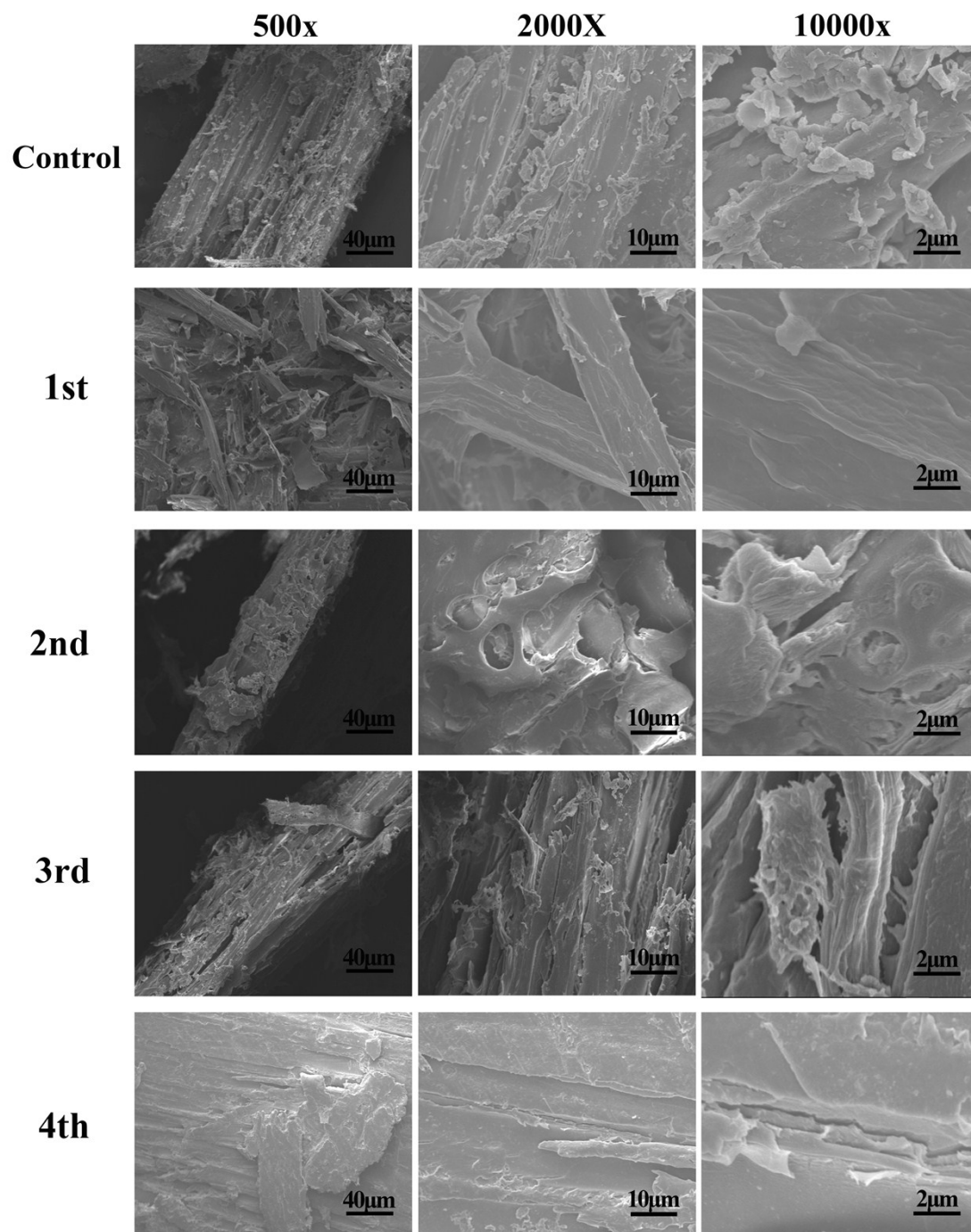


Figure S15. SEM images of original and the pretreated substrates under different pretreatment cycle times.

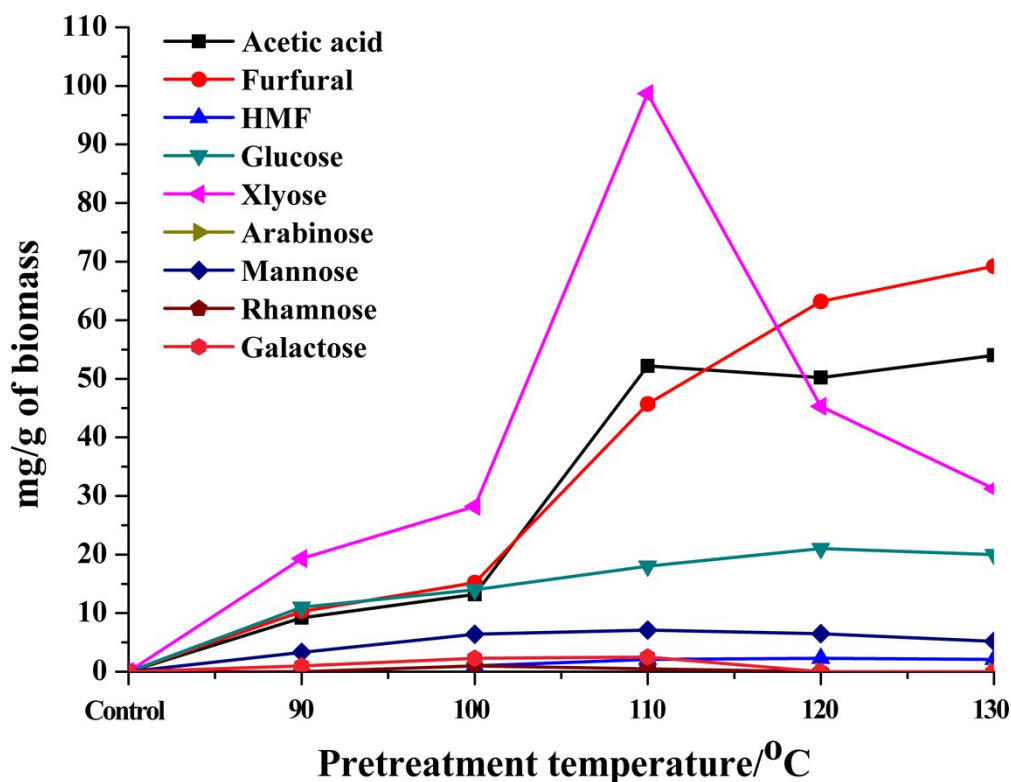


Figure S16. Inhibitors and monosaccharides in the DES solution after the different pretreatment temperatures

Compositional analysis of the cellulose-rich substrates showed that the majority of the hemicelluloses have been dissolved into the DES solution. In addition, the subsequent 2D-HSQC NMR spectra showed that the dissolved hemicelluloses do not involve in the regenerated lignin. In fact, pentose (xylose, arabinose, mannose, rhamnose) were degraded into furfural and further into formic acid, while the decomposition of hexose (glucose, galactose) resulted in the formation of HMF and further to formic acid as well as levulinic acid. Meanwhile, acetic acid was typically generated from the cleavage of the acetyl groups in the hemicelluloses components.

Figure S16 shows the amount of solutes detected in the DES solution during the pretreatment. The amount of monosaccharide (xylose, galactose, arabinose, mannose,

rhamnose) in the liquid phase was increased at 110 °C. For example, the maximum amount of xylose detected in the liquor at 110 °C was ca. 10% of the total biomass and ca. 50% of the xylan. The maximum removal of hemicelluloses will facilitate the enzymatic saccharification. After 110 °C, the xylose concentration in the DES solution decreased due to the degradation. The furfural content in the liquor increased with pretreatment temperature. The acetic acid concentration increased as the temperature increased to 110 °C and subsequently remained stable. Once the concentration constant, it was found that the concentration of acetic acid reached to about 50 mg/g biomass. Besides, it is noteworthy that only small quantities of glucose were detected in the DES solution, suggesting that cellulose is stable during the pretreatment.

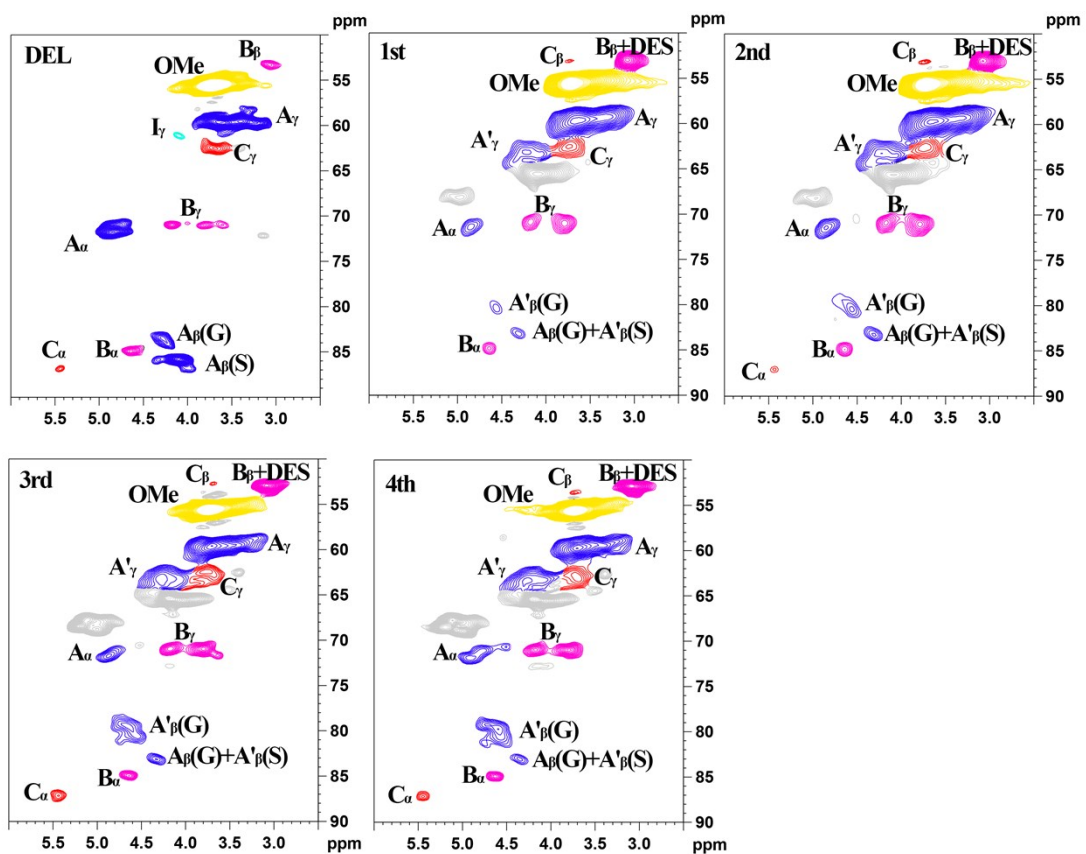


Figure S17. Side-chain in the 2D HSQC NMR spectra of DEL and the lignins obtained under different pretreatment cycles.

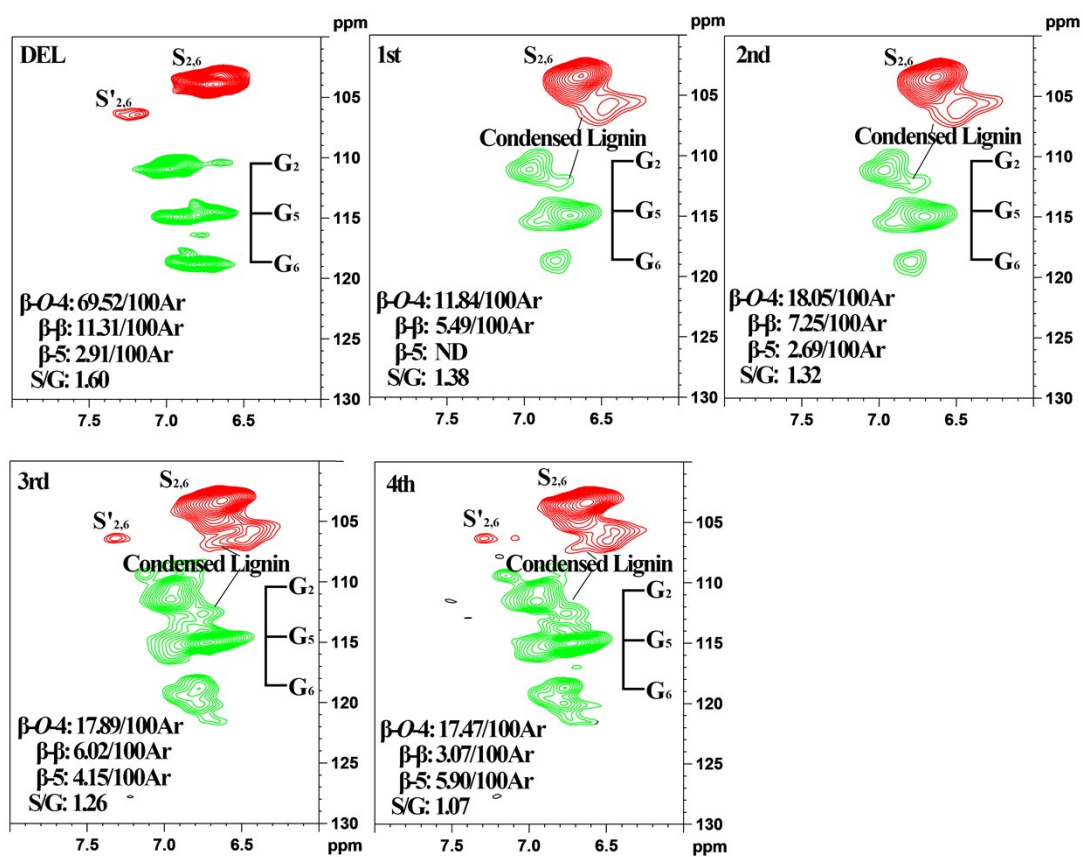


Figure S18. Aromatic region in the 2D HSQC NMR spectra of DEL and the lignins obtained under different pretreatment cycles.

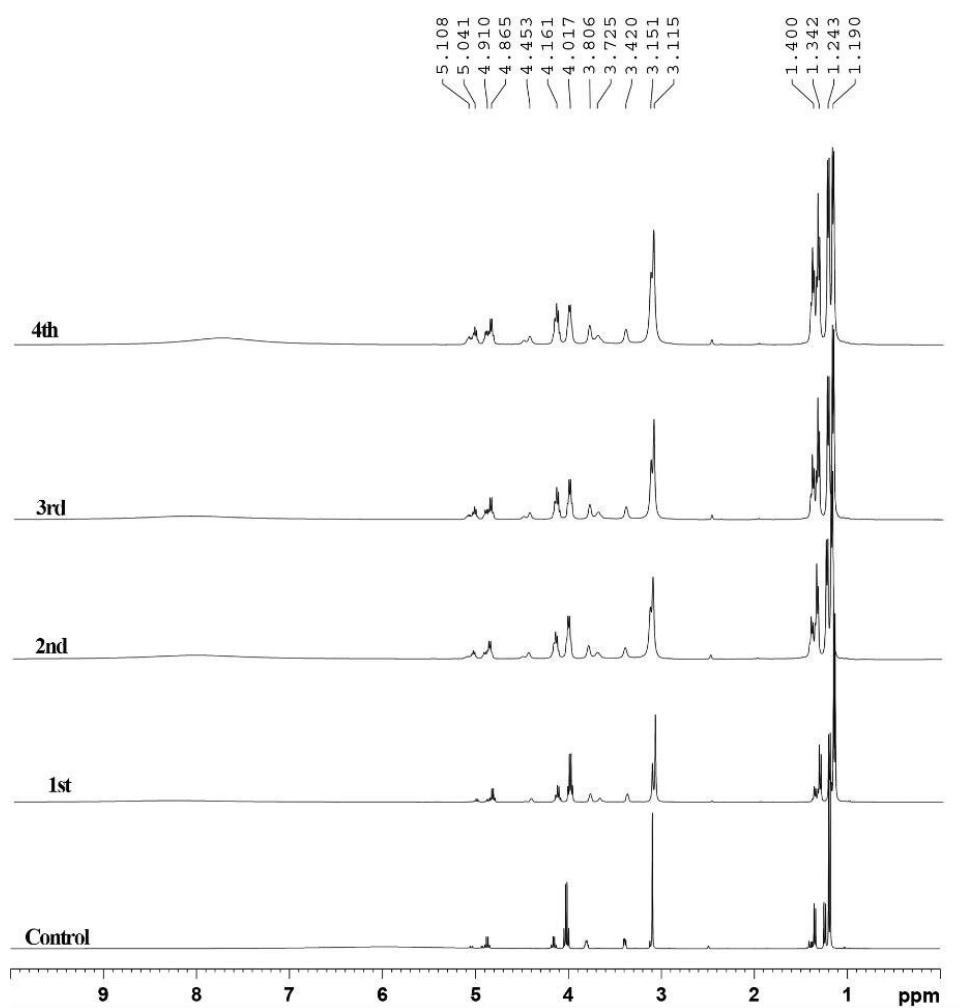


Figure S19. ¹H NMR spectra of fresh and the recycled DES at different DES cycles.

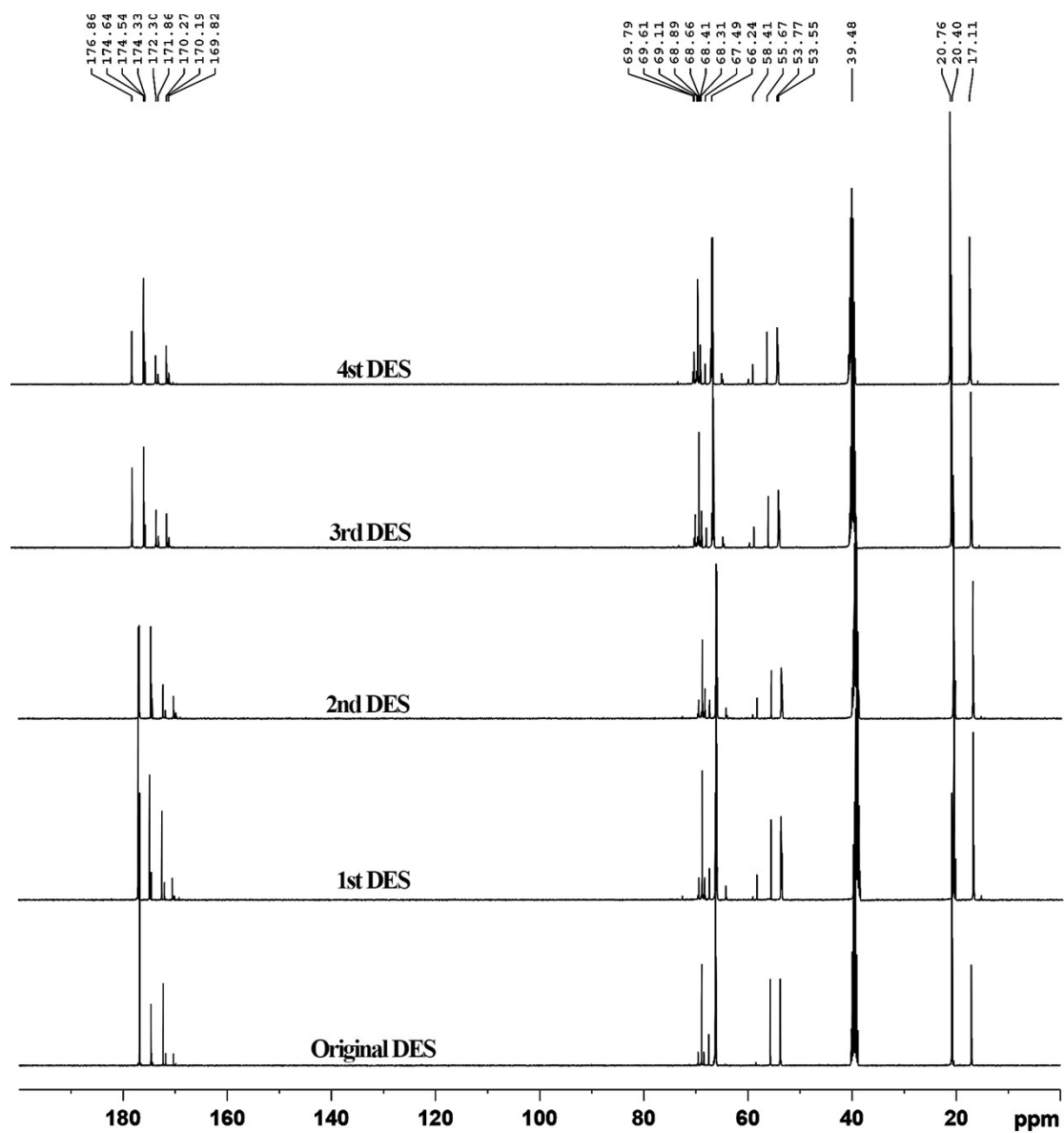


Figure S20. ^{13}C NMR spectra of fresh and the recycled DES at different DES cycles

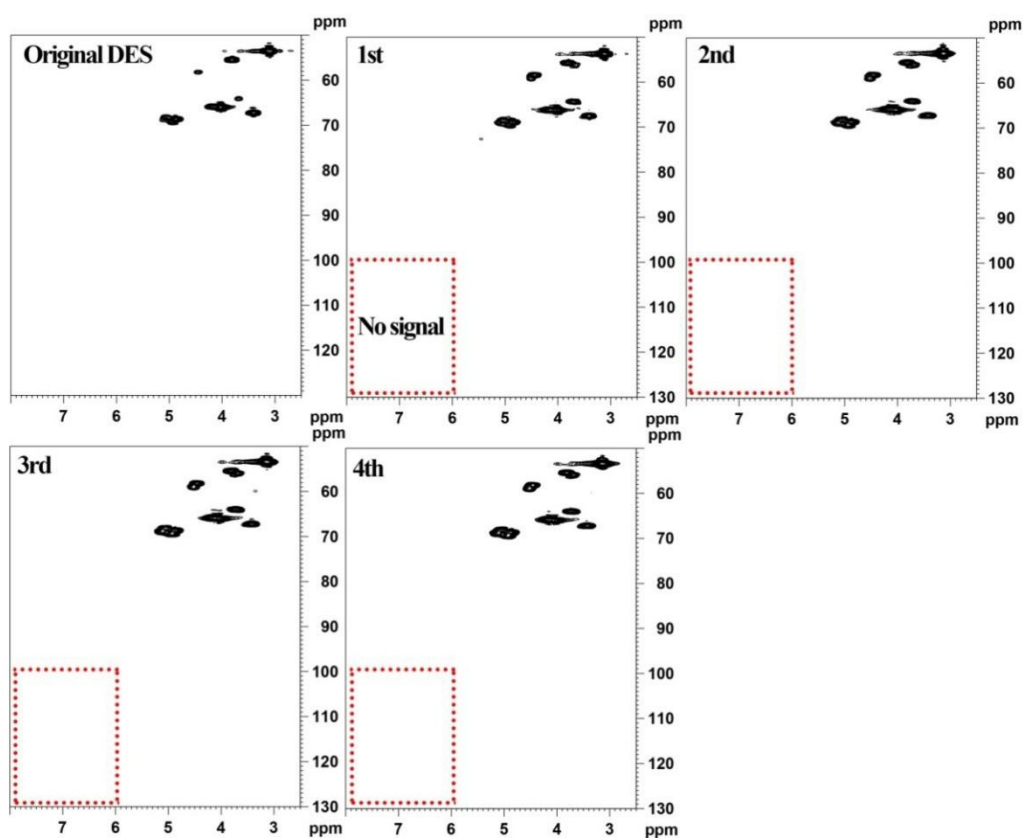


Figure S21. 2D-HSQC NMR spectra of fresh and the recycled DES at different DES cycles.

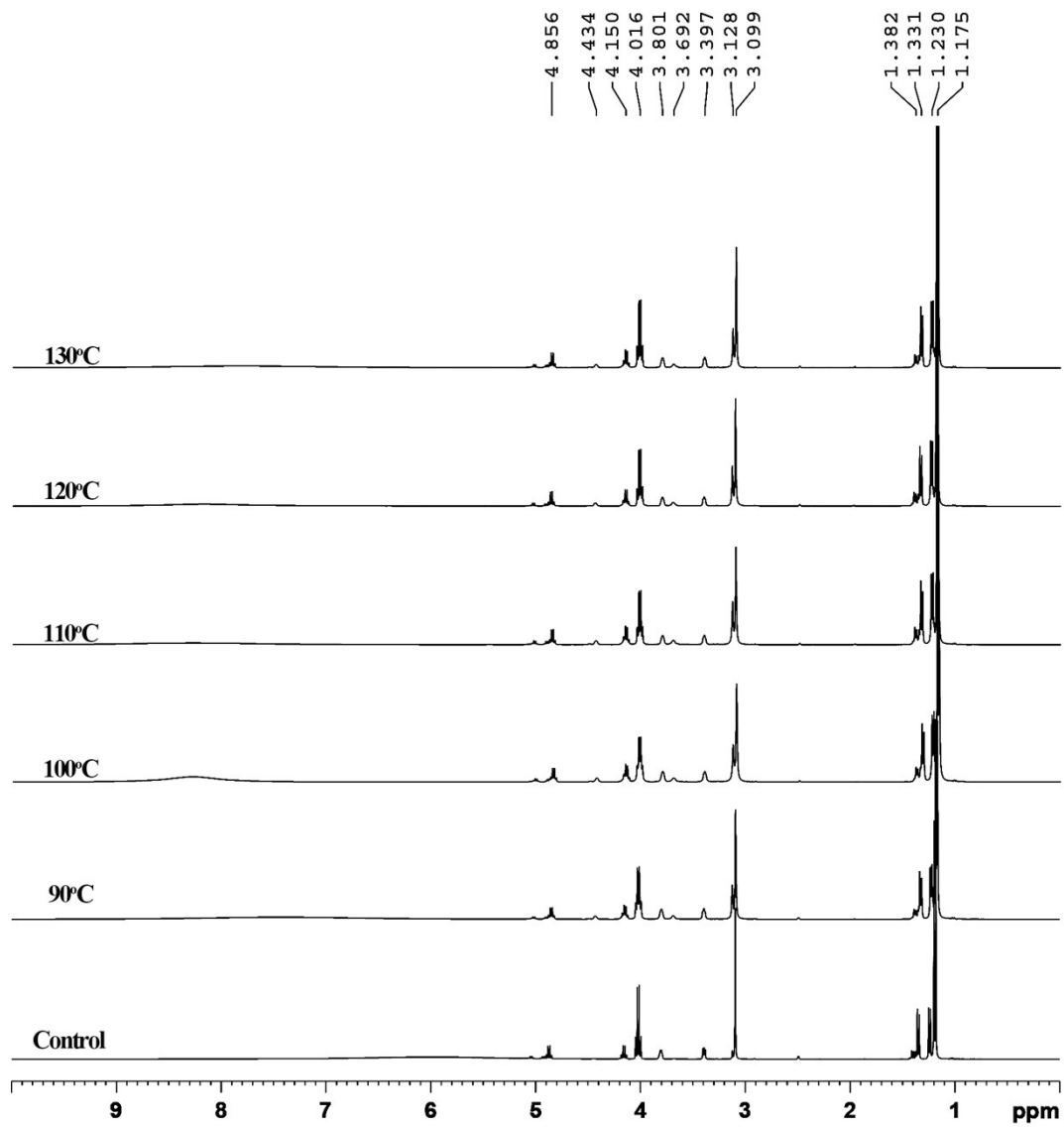


Figure S22. ^1H NMR spectra of fresh and the recycled DES under different pretreatment temperatures.

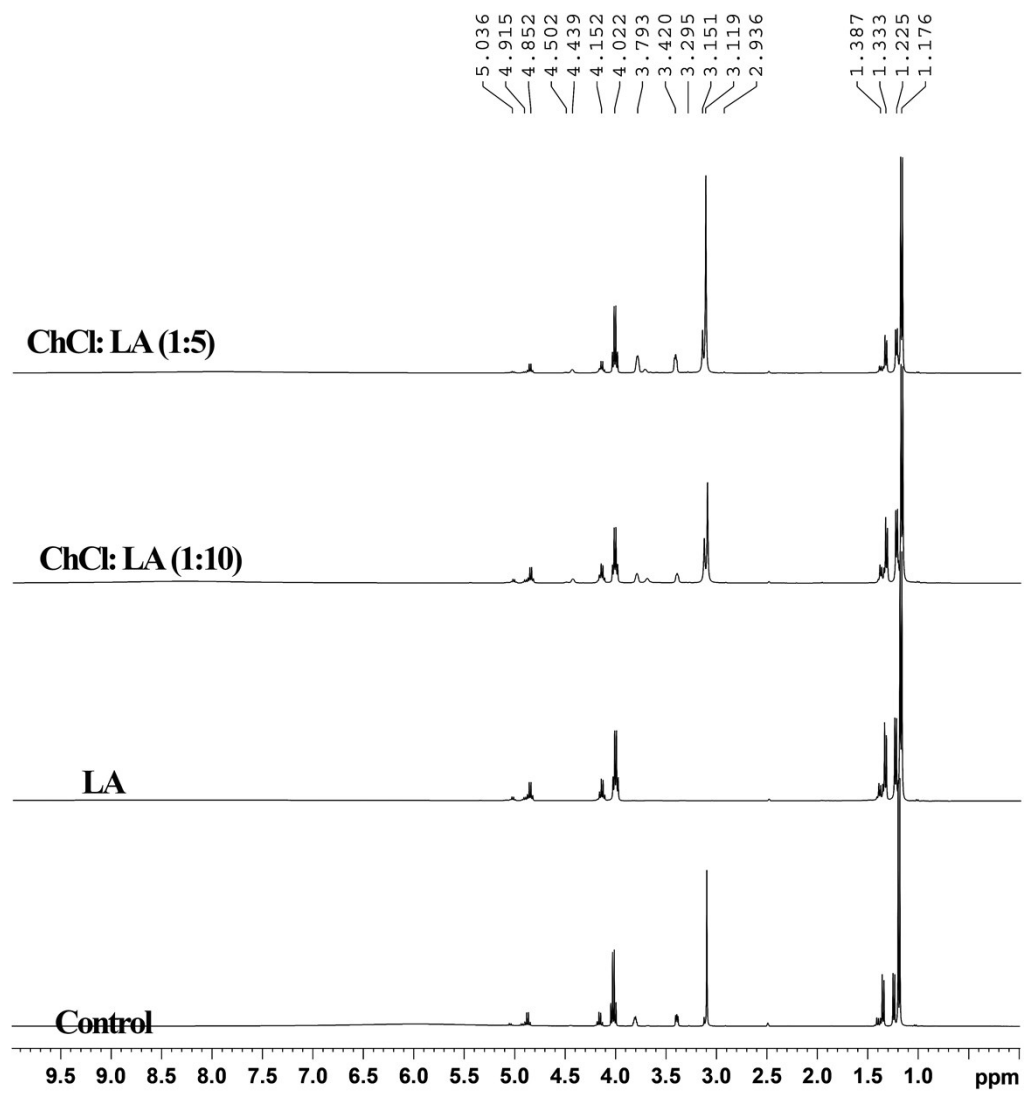


Figure S23. ^1H NMR spectra of fresh and the recycled DES at different DES ratio.

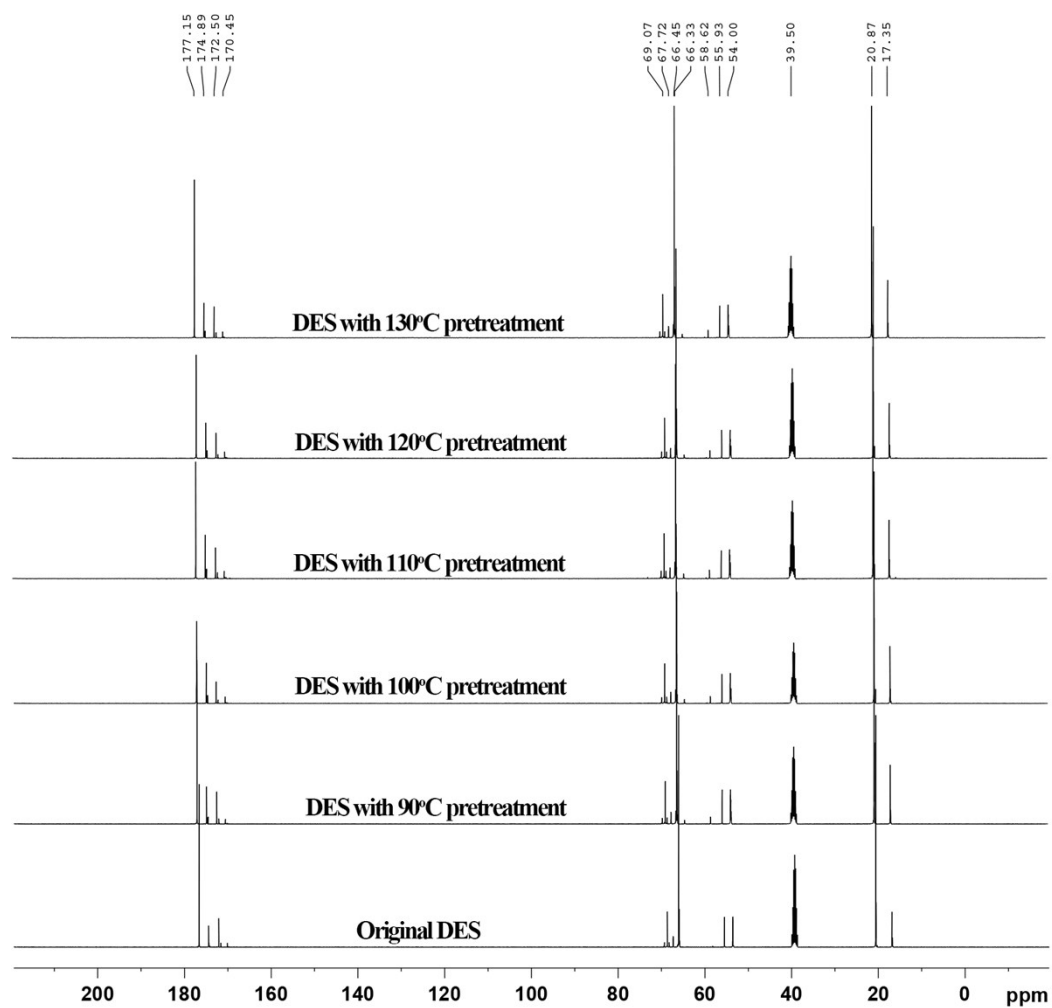


Figure S24. ^{13}C NMR spectra of fresh and the recycled DES under different pretreatment temperatures

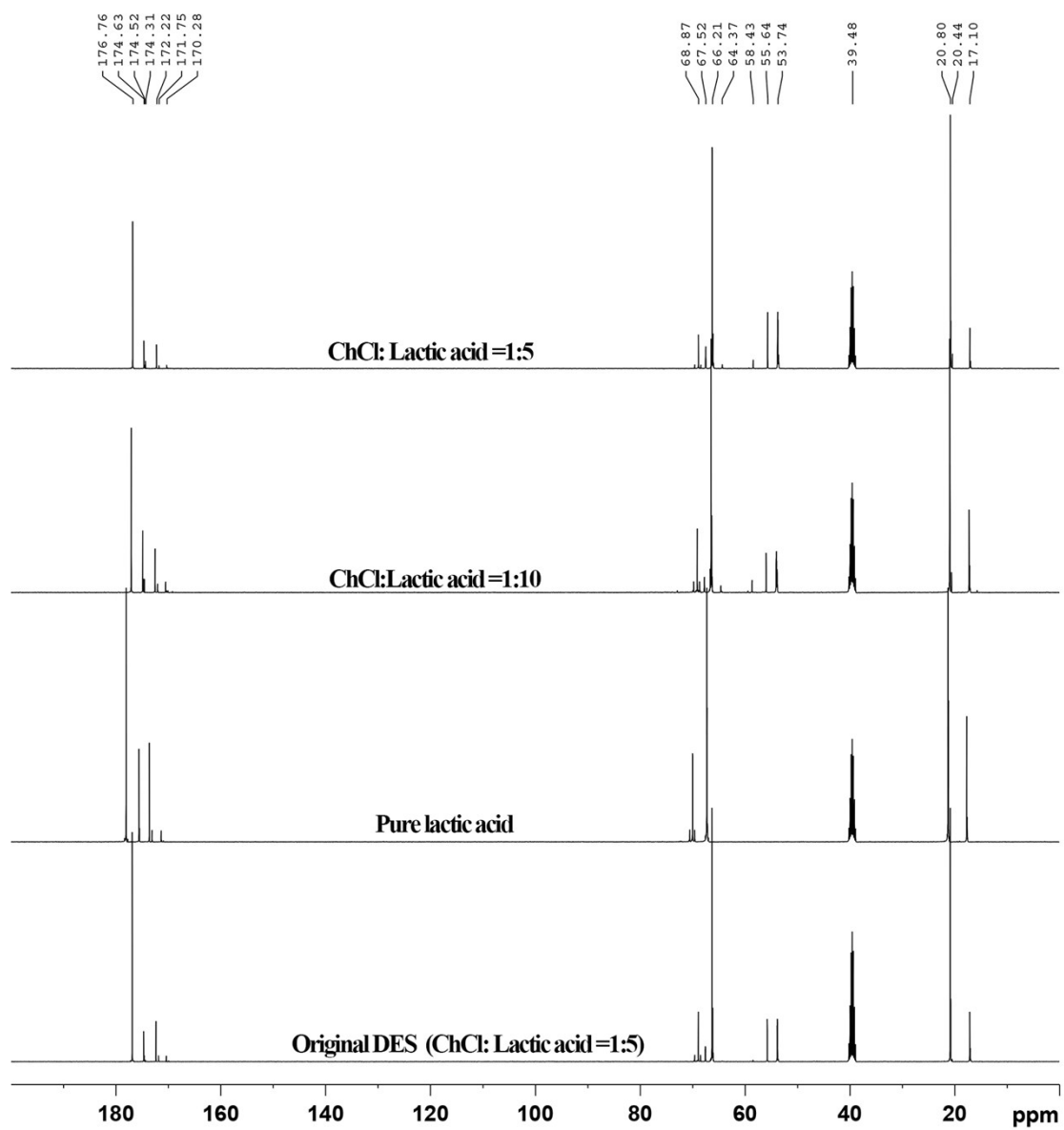


Figure S25. ^{13}C NMR spectra of fresh and the recycled DES at different DES ratio.

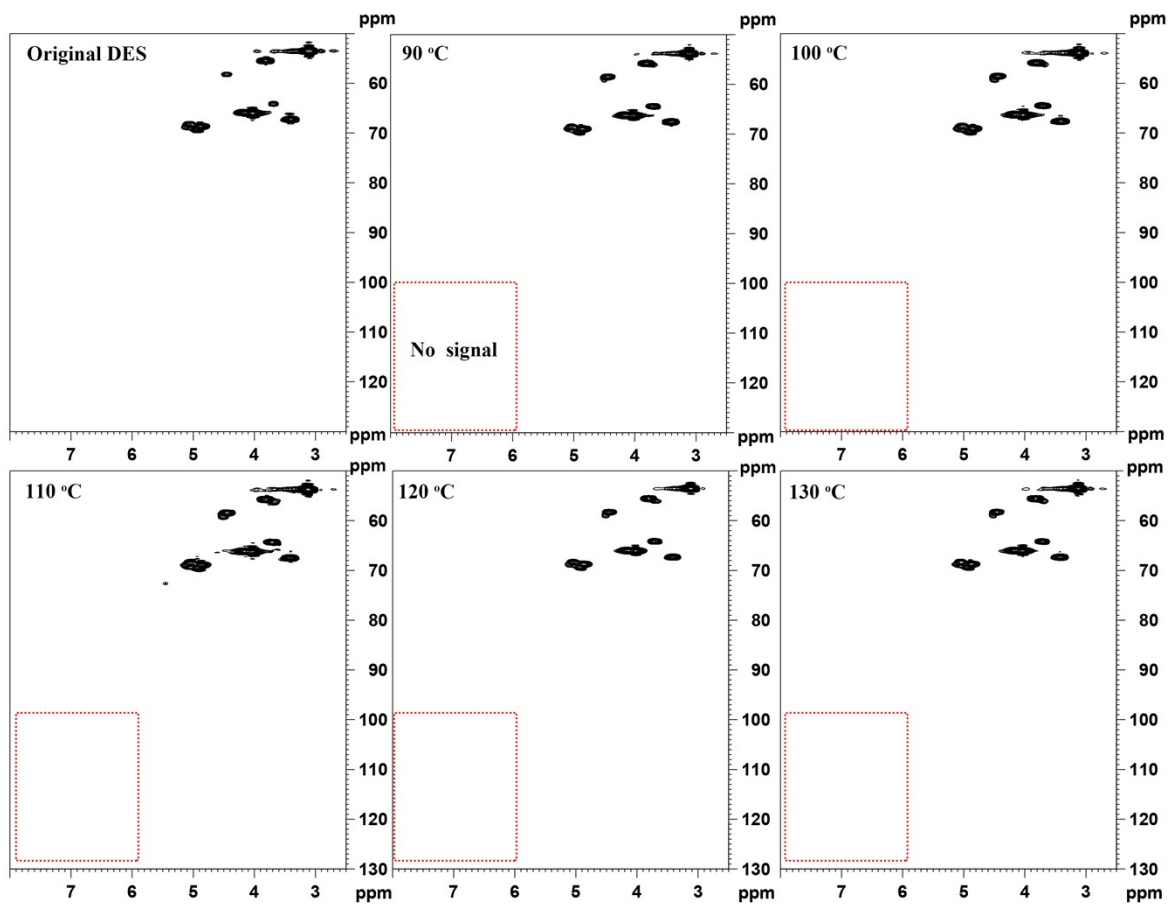


Figure S26. Side-chain and aromatic region in the spectra of pure DES and the recycled DES under different pretreatment temperatures

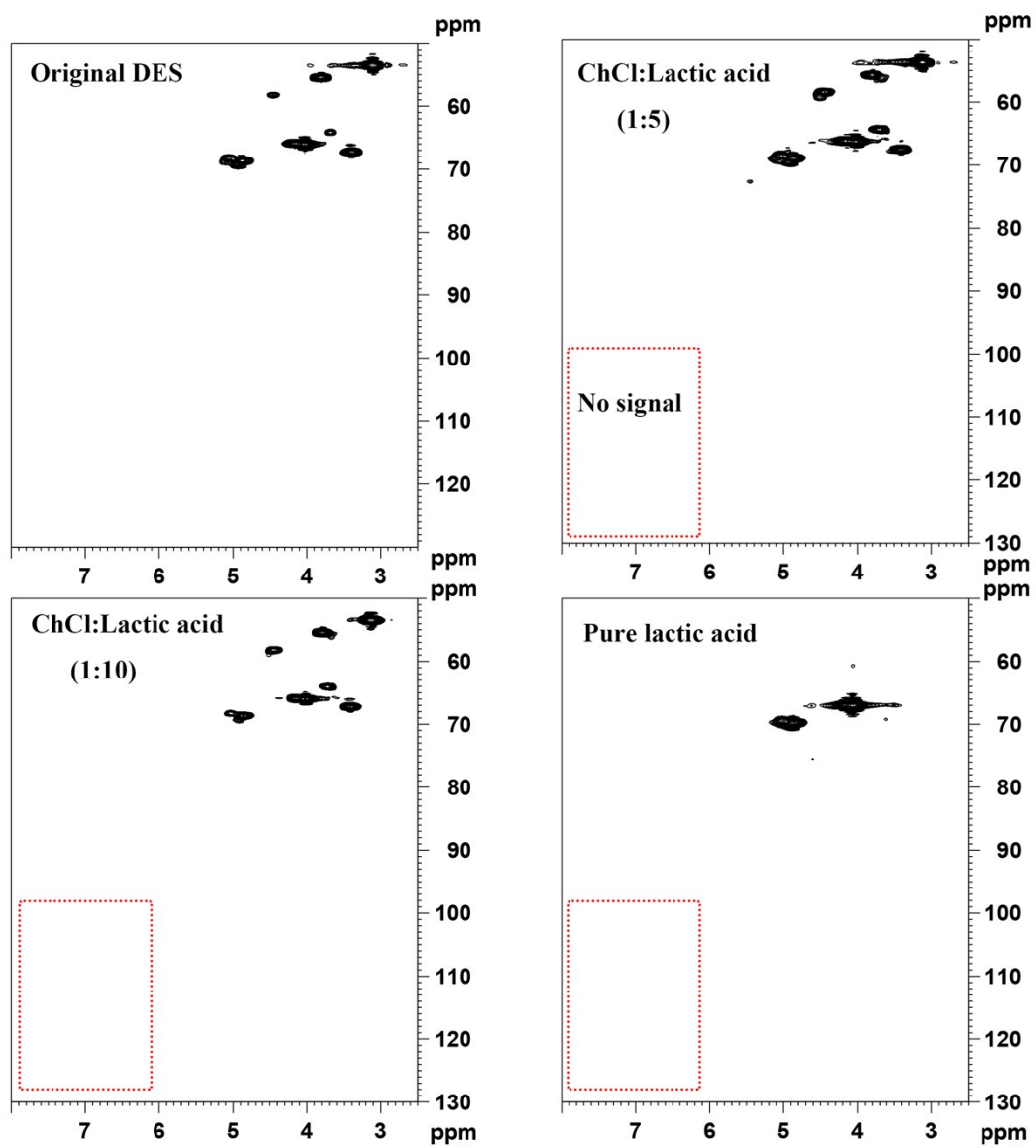


Figure S27. Side-chain and aromatic region in the 2D HSQC NMR spectra of pure DES and the recycled DES under different DES ratio.

Reference

- Crestini, C., Argyropoulos, D.S. 1997. Structural Analysis of Wheat Straw Lignin by Quantitative ^{31}P and 2D NMR Spectroscopy. The Occurrence of Ester Bonds and α -O-4 Substructures. *Journal of Agricultural and Food Chemistry*, **45**(4), 1212-1219.
- Pu, Y., Cao, S., Ragauskas, A.J. 2011. Application of quantitative ^{31}P NMR in biomass lignin and biofuel precursors characterization. *Energy & Environmental Science*, **4**(9), 3154.
- Segal, L.C., Creely, J., Martin, A.E.J., Conrad, C.M. 1959. An Empirical Method for Estimating the Degree of Crystallinity of Native Cellulose Using the X-Ray Diffractometer. *Textile Research Journal*, **29**(10), 786-794.
- Shen, X.-J., Wang, B., Pan-li, H., Wen, J.-L., Sun, R.-C. 2016a. Understanding the structural changes and depolymerization of Eucalyptus lignin under mild conditions in aqueous AlCl_3 . *RSC Advances*, **6**(51), 45315-45325.
- Shen, X.J., Wang, B., Huang, P.L., Wen, J.L., Sun, R.C. 2016b. Effects of aluminum chloride-catalyzed hydrothermal pretreatment on the structural characteristics of lignin and enzymatic hydrolysis. *Bioresource Technology*, **206**, 57-64.
- Wen, J.-L., Sun, S.-L., Yuan, T.-Q., Sun, R.-C. 2015. Structural elucidation of whole lignin from Eucalyptus based on preswelling and enzymatic hydrolysis. *Green Chem.*, **17**(3), 1589-1596.